A NEW TWO-COLOR INFRARED PHOTODETECTOR DESIGN USING INGAAS/INALAS COUPLED QUANTUM WELLS

August 1999

J. W. Little,[1] S. W. Kennerly, R. P. Leavitt, M. L. Lucas, and K. A. Olver
IR Materials Branch, U. S. Army Research Laboratory
Adelphi, MD 20783

ABSTRACT

We have grown, fabricated, and tested a new two-color quantum well infrared photodetector (QWIP) that uses coupled pairs of InGaAs/InAlAs wells grown lattice matched to an InP substrate. A set of wells with a peak response at about 8 μm was vertically integrated with a set responding at about 4μm. Top, bottom, and intermediate contact layers were included to allow for independent biasing and photocurrent readout. Unlike currently available two-color QWIPs using strained InGaAs wells in the mid-wave section, all the layers in this design are nominally strain-free. The long-wave portion uses 20 periods of coupled InGaAs wells with superlattice barriers, and the mid-wave portion has 10 periods of coupled InGaAs wells with uniform InAlAs barriers. The coupled-well design gives enhanced absorption per unit thickness compared with single-well structures, and allows the number of quantum well periods (and thus the total device thickness) to be reduced. This should lower operating biases and improve the efficiency of conventional gratings used as optical coupling structures. We give the results of 78-K radiometric tests on 8 x 8 pixel arrays that show uniform background-limited performance and relatively high conversion efficiencies in the mid-wave band. The long-wave band is partially background limited at 78 K. The magnitude of the mid-wave response at 78 K was found to depend on the frequency of the chopper used on the blackbody source, but this dependence vanished at higher detector temperatures. We discuss a possible source for the frequency dependence and suggest design modifications to eliminate it.

1.0 INTRODUCTION

The U. S. Army Research Laboratory (ARL), in collaboration with a number of industry and university partners, is developing a new generation of sensors that can perform advanced signal processing functions over a very wide range of wavelengths (e.g., from the ultraviolet to the millimeter-wave region of the spectrum). Part of this new sensor concept, known as the multi-domain smart sensor (MDSS), requires the development of infrared focal plane arrays (FPAs) that image simultaneously in two or more wavelength bands. These FPAs would be very useful for identifying targets and defeating countermeasures and would widen the range of atmospheric conditions over which high-quality imaging could be performed (e.g., fog, smoke, etc.).

Quantum well infrared photodetectors (QWIPs) based on III-V semiconductor materials are well suited for application to dual-band imagers because the operating wavelength can be varied over a large range that spans the mid-wave infrared (MWIR) and the long-wave infrared (LWIR) atmospheric transmission windows of 3 to 5 and 8 to 12 μm, respectively. Molecular beam epitaxy (MBE) can be used to sequentially grow the layers that comprise the different sections of a dual-band QWIP on a common substrate. This leads to natural pixel registration in an FPA application. QWIP FPAs operating in two LWIR bands have been demonstrated,[2] and, recently, the first two-

[1] Also with the Electrical Engineering Dept., University of Maryland, College Park.
[2] M. Sundaram, et al., "Advances in QWIP FPA Technology," Proc. 1998 IRIS Specialty Group on Detectors, 1999.

Form SF298 Citation Data

Report Date *("DD MON YYYY")* 00081999	**Report Type** N/A	**Dates Covered (from... to)** *("DD MON YYYY")*

Title and Subtitle A New Two-Color Infrared Photodetector Design Using INGAAS/INALAS Coupled Quantum Wells	**Contract or Grant Number**
	Program Element Number
Authors	**Project Number**
	Task Number
	Work Unit Number
Performing Organization Name(s) and Address(es) IR Materials Branch U. S. Army Research Laboratory Adelphi, MD 20783 &	**Performing Organization Number(s)**
Sponsoring/Monitoring Agency Name(s) and Address(es)	**Monitoring Agency Acronym**
	Monitoring Agency Report Number(s)
Distribution/Availability Statement Approved for public release, distribution unlimited	
Supplementary Notes	
Abstract	
Subject Terms	
Document Classification unclassified	**Classification of SF298** unclassified
Classification of Abstract unclassified	**Limitation of Abstract** unlimited
Number of Pages 15	

color FPA with simultaneous readout of an LWIR (9-μm peak) and an MWIR (5.1-μm peak) band was tested[3] and shown to provide high-quality images.

2.0 PERFORMANCE ISSUES

The most challenging part of the development of a dual-band LWIR/MWIR QWIP has been the MWIR section[4] because it requires much deeper quantum wells than those normally grown in the standard GaAs/AlGaAs QWIP system. The high aluminum mole fractions required for MWIR intersubband transitions generally result in poor barrier material quality (deep-level traps, low mobility, etc.). Two alternative material systems for MWIR operation are strained InGaAs/AlGaAs quantum wells grown on GaAs substrates and InGaAs/InAlAs grown lattice-matched (unstrained) on InP substrates. The two-color detector studied by Goldberg, et al., uses the strained InGaAs/AlGaAs system for the MWIR section. Field tests of imaging with this array[5] indicate that the 5.1-μm peak operating wavelength is too long to give the full advantage of the two-color imaging (i.e., strong contrast between the two images is not present). The ideal MWIR section should operate at about 4 μm with a long-wavelength cutoff below the 4.2-μm carbon dioxide atmospheric absorption line. Operating wavelengths as low as 4.3 μm have been observed in the strained InGaAs system[4], but this design required a high indium mole fraction (yielding a highly strained well) and a high aluminum mole fraction (close to the indirect-gap transition, which is known to have inferior material quality).

Calculations[4] have shown that the InGaAs/InAlAs system that is grown lattice-matched to InP substrates should give operating wavelengths just below 4 μm, with absorption strengths substantially larger than the strained systems. We have measured MWIR InGaAs/InAlAs QWIPs with peak operating wavelengths of about 4.1 μm. Single-pixel tests have shown that devices from some wafers show very low dark current and relatively high responsivity at 78 K. However, other wafers grown using the same recipe have shown high dark currents that varied from pixel to pixel with a range of 1 to 2 orders of magnitude. Figure 1 shows temperature-dependent dark current measurements (i.e., with a cold shield covering the aperture in the dewar) on a sample of this type. Note that at

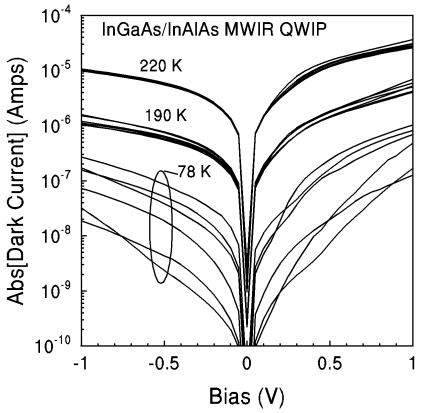

Figure 1. Temperature-dependent dark current measurements on an InGaAs QWIP showing low-temperature nonumiformity.

higher temperatures, the currents are uniform; but at 78 K, each pixel had a different dark current, and the values

[3] A. Goldberg, et al., "Dual Band MWIR/LWIR Focal Plane Array Test Results," to be published, Proc. 1999 IRIS Specialty Group on Detectors.
[4] M. Z. Tidrow, J. W. Little*, R. P. Leavitt, A. C. Goldberg*, S. W. Kennerly, P. N. Uppal, and M. Sundaram, "Mid-Wavelength Quantum Well Infrared Photodetectors," Proc. 1998 IRIS Specialty Group on Infrared Materials, 1999.
[5] A. C. Goldberg, private communication.

were all substantially higher than would be expected for thermal activation from the deep well of an MWIR detector. We have tentatively correlated the high, nonuniform dark current with the presence of three-dimensional (rough) morphology on the surface of the wafer. This morphology is indicative of the relief of tensile strain in the thick epilayers. X-ray diffraction measurements on other samples that have shown the high dark current support the assumption that the layers were under tensile strain. Because of the relatively thick epilayers required for a QWIP (particularly a two-color QWIP), a high degree of accuracy in the composition of the layers is critical. Any design modifications that reduce the thickness of the total growth would help to ensure high-quality crystal growth.

Another issue that must be taken into account with any two-color QWIP structure is the coupling of the infrared radiation into both bands. This is currently accomplished using a rectangular grating that is etched into the top contact and coated with metal to form a reflection grating. The grating period in one direction couples the LWIR light and a shorter period in the other direction couples the MWIR light into the chip. This two-color QWIP was designed with the MWIR section on the bottom and the LWIR section on the top. This design was chosen to minimize the dark current in the LWIR section, since during the processing of the pixels, the top layer has the most area removed to allow for contacting underlying layers. However, Beck, et al.,[6] showed that the evanescent part of the optical fields (which can contribute substantially to the optical coupling) falls off more rapidly with distance from the grating for the MWIR component than for the LWIR component of the grating. This would suggest that the MWIR layer should be placed closer to the grating (i.e., on the top). It was also shown that due to finite pixel size effects, it is better to have all the absorbing quantum wells as close to the grating as possible.

3.0 DETECTOR DESIGN, GROWTH, AND FABRICATION

Based on the promising results that we obtained on a new LWIR QWIP structure containing coupled quantum wells,[7] we developed a new two-color design that addresses many of the issues described above. Coupled pairs of quantum wells are used instead of single isolated wells in each period of the structure in to increase the absorption per period. This leads to a thinner detector structure that should be easier to grow in the InGaAs/InAlAs system without lattice relaxation, and it places the absorbing quantum wells closer to the diffraction grating, as recommended by Beck, et al.

Figure 2 shows the basic detector design with the layer thicknesses, compositions, and doping densities labeled. To match the lattice constant of the InP substrate, all InGaAs layers have an indium mole fraction of 0.53, and all InAlAs layers have an indium mole fraction of 0.52. Details of the theoretical model and materials parameters used in the design will be described elsewhere.[8] We will give only the salient characteristics here.

The LWIR section consists of 20 doped, coupled InGaAs quantum well pairs (80-Å each, separated by a 30-Å InAlAs barrier), with each pair of wells surrounded by InGaAs/InAlAs superlattice barriers (with a total superlattice barrier thickness of 484 Å). The total two-dimensional doping density is 6.4×10^{11} cm^{-2} in each period. The well widths and coupling barrier thicknesses were chosen so that the two dominant intersubband transitions characteristic of the coupled-well system[8] would be at about 7.5 and 8.5 μm. The overall response would, therefore, be a convolution of these two transitions. The superlattice layer thicknesses were chosen to provide a miniband of electronic states with the lowest energy state coincident with the excited states of the coupled wells. This is the InGaAs/InAlAs embodiment of the GaAs/AlGaAs coupled QWIP described by Kennerly et al. This basic QWIP design is referred to as a bound-to-miniband[9] or a miniband transport[10] (MBT) detector. Since the composition (and

---

[6] W. A Beck, M. S. Mirotznik, and P. N. Uppal, "Design of QWIP Optical Coupling Structures for MDSS," Proc. 2nd Annual Fedlab Symposium, College Park, MD, 1998.

[7] S. W. Kennerly, D. W. Beekman, J. W. Little, A. C. Goldberg, and R. P. Leavitt, "Comparison of Single Well and Double and Triple Coupled Quantum Well Infrared Detector Designs," 1998 IRIS Specialty Group on Detectors, 1999.

[8] J. W. Little, R. P. Leavitt, S. W. Kennerly, A. C. Goldberg, manuscript in preparation.

[9] L. S. Yu and S. S. Li, Appl. Phys. Lett. **59**, 1332, 1991.

[10] W. A. Beck, J. W. Little, A. C. Goldberg, and T. S. Faska, "LWIR Imaging Using Miniband Transport Quantum Well Infrared Detectors," Symposium Proceedings: Electrochemical Society, October 1993.

thus the bandgap) of the high-bandgap material (i.e., the InAlAs) must remain fixed (to match the substrate lattice constant), the MBT design is required for LWIR operation in this material system. The miniband provides a conducting channel for the extraction of photocarriers residing in the deeply bound excited states of the 80-Å wells.

The MWIR section comprises 10 doped, coupled InGaAs quantum well pairs (34-Å each, separated by a 50-Å InAlAs barrier), with each pair of wells surrounded by 400-Å thick InAlAs barriers. The total two-dimensional doping density is 6.8×10^{11} cm^{-2} in each period. This system was designed to have the dominant transitions at about 3.8 and 4.1 μm, with the shorter wavelength transition broadened by coupling of the higher-energy excited state to the states in the InAlAs conduction band continuum. This basic design is referred to as a bound-to-quasibound (BQB)[11] QWIP since the excited states are very close in energy to the top of the barrier and are, therefore, nearly unbound.

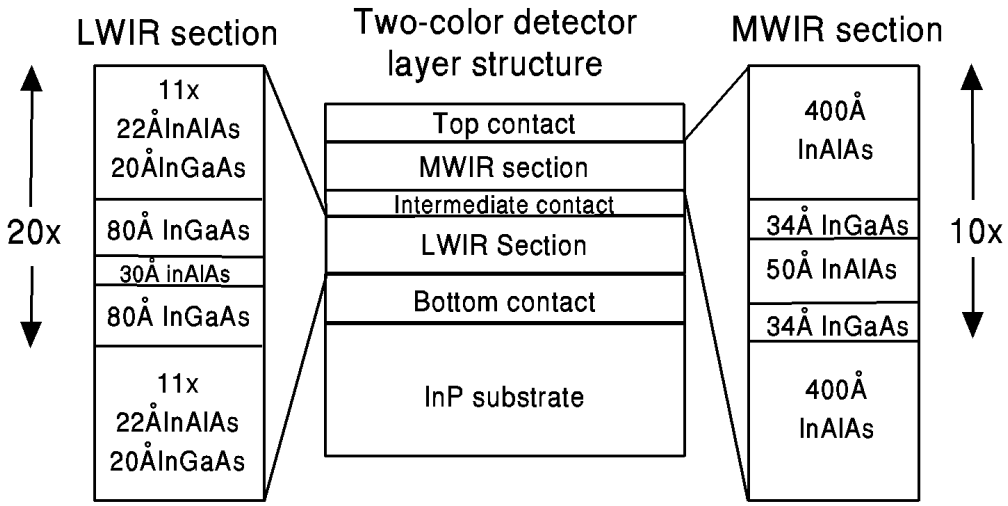

Figure 2. Two-color QWIP layer structure.

The LWIR and MWIR sections are separated by a 0.5-μm doped InGaAs intermediate contact layer. A 1.5-μm doped InGaAs bottom contact is between the semi-insulating InP substrate and the LWIR section, and a 0.75-μm doped InGaAs top contact is above the MWIR section. In a grating-coupled FPA, this top contact would be etched and metalized to form a diffraction grating for infrared light incident from the substrate side of the array.

The detector design described above gives active region thicknesses for both bands that are about 60% of the thicknesses of isolated-well devices with the same number of quantum wells (i.e., with one well per period and twice the number of periods). Thus, in a grating-coupled array, the wells will be closer to the top surface that contains the diffraction grating. As mentioned above, this should improve the overall efficiency of the optical coupling into both bands. The MWIR section was placed closest to the top and was limited to 10 periods to try to maximize the coupling between the absorbing wells and the rapidly decaying evanescent fields of the MWIR component of the diffraction grating.

A wafer containing the layer structure described above was grown on a 2-in. semi-insulating InP substrate using MBE. A companion wafer was also grown in which the coupled pairs of quantum wells were replaced with single, isolated wells of the same thickness (i.e., single 80-Å wells for the LWIR section and 34-Å wells for the MWIR

[11] S. D. Gunapala, J. K. Liu, J. S. Park, M. Sundaram, C. A. Shott, T. Hoelter, T-L. Lin, S. T. Massie, P. D. Maker, R. E. Muller, and G. Saursi, IEEE Trans. On Elect. Dev. **44** (1), 51 (1997).

section). The companion sample is used as a standard with which to compare the properties of the coupled-well detector. The surface morphology of both wafers was flat and specular with very few oval defects. X-ray diffraction measurements showed that the residual strain in the epilayers is comparable to AlGaAs with an aluminum mole fraction of about 0.25 grown on a GaAs substrate. This indicates that the detector structures should be essentially strain-free and of high crystal quality.

In the following sections, we will give preliminary results of radiometric tests on 8 x 8 arrays of detectors pixels designed to allow independent biasing of and photocurrent readout from the two sections of each pixel. Figure 3 shows a schematic (left) of a two-color detector and an electron micrograph (right) of a 100 x 100-μm^2 pixel with indium bumps on the top and the intermediate contacts. The ground plane common contact is outside of the field of view of the micrograph. On the devices tested here, the percentage of the area etched away from the top (MWIR) layer to make the intermediate contact ranged from 4% to 8%, depending on the total area of the pixel.

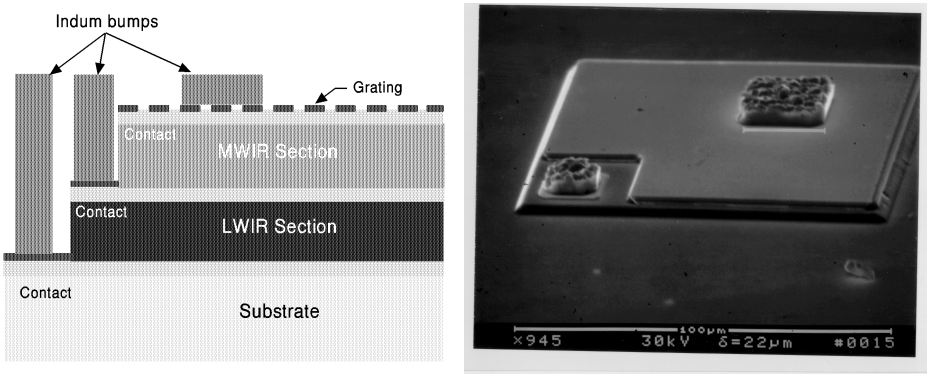

Figure 3. Schematic (left) of a two-color pixel and an electron micrograph (right) of a 100 x 100 micron square pixel with indium bumps on the top and the intermediate contacts.

The photomask set used to process the two-color detectors contained arrays in which all of the pixels were 100-μm squares and arrays in which the pixels varied from 200-μm squares to 20-μm squares. The constant-area arrays were used to test for uniformity of dark current and responsivity. The second type can be used to check for the scalability of some parameters to the area to look for effects such as scattering of light from the edges of the pixels. In both types of arrays, the pixels were arranged on a 200-μm center-to-center square grid. Individual arrays were diced from the wafer using a diamond-blade dicing saw. A facet was polished (at a 45° angle to the top surface) in one side of the chip, and the array was bonded to a silicon fanout chip using a flip-chip hybrid bump bonder to mate the indium bumps on each pixel to equivalent bumps on the fanout (as shown in fig. 4). This facet provides an essentially wavelength-independent way of converting the normally incident, unpolarized light from a Fourier-transform infrared (FTIR) spectrometer or a calibrated blackbody source into nonnormally incident light with a component of polarization that is perpendicular to the plane of the quantum wells as required by the selection rules for intersubband absorption.[12] On most of the chips, an epoxy was wicked between the detector and the fanout chip to provide mechanical stability. The hybrid chip was mounted in a leadless chip carrier (LCC), and wire bonds from the chip to the pads of the LCC provided electrical access to the individual contacts on the two-color pixels. The LCC was then mounted in a pour-fill liquid nitrogen dewar for radiometric tests at about 78 K.

[12] L. C. West and S. J. Eglash, Appl. Phys. Lett. **46**, 1156 (1985).

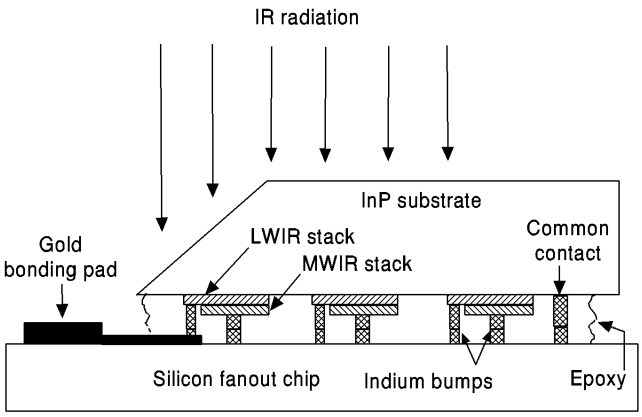

Figure 4. Schematic of detector chip hybridized to a silicon fanout chip,

4.0 SPECTRAL CHARACTERISTICS

As was mentioned in section. 2.0, epoxy is sometimes used to mechanically stabilize the hybridized detector/fanout chip. Since most epoxies contain organic compounds with absorption lines in the infrared, the presence of the epoxy in contact with certain detector surfaces can have a dramatic effect on the spectral response of the detector. This is because absorption by the epoxy can substantially affect the spectral distribution of the radiation that is incident on the detector pixels. This is particularly true for these two-color detectors, since the photomasks were designed such that only a small region around the indium bumps is coated with ohmic metal (that would separate the epoxy from the detector surface). The majority of the pixel surface is not metal-coated and, therefore, comes in contact with epoxy that is wicked between the detector and the fanout chips. Figure 5 shows the relative photoresponse of the LWIR section of one of the single-well detectors before (top) and after (bottom) epoxy was applied. The strong, irregularly spaced dips in the spectrum of the epoxy-wicked sample are due to absorption

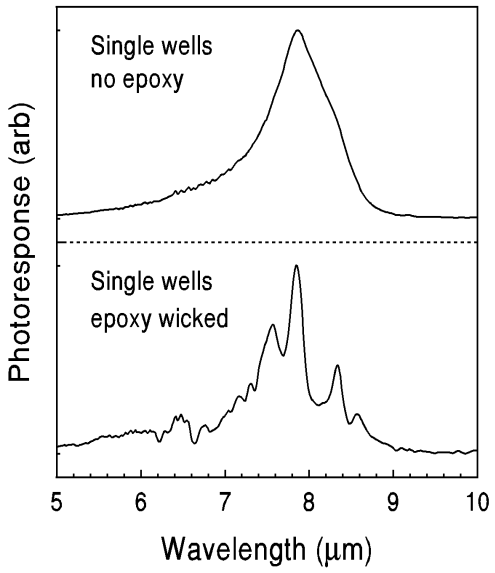

Figure 5. Relative response of a single-well LWIR QWIP before (top) and after (bottom) eposy was applied.

of infrared light by the epoxy, and are only observed for wavelengths longer than about 6 μm. Although a properly designed pixel for use in FPA applications would minimize the exposure of any surfaces to the epoxy, we must be aware that for the experiments described here, the magnitudes of LWIR radiometric parameters that depend on the intensity of the incident light (e.g., responsivity, detectivity, quantum efficiency, etc.) are reduced compared with the same detectors in the absence of the epoxy.

Figure 6 shows the relative photocurrent response versus wavelength for the LWIR sections of the single-well (a) and the coupled-well (b) samples at a bias of –2 V. For these and all other measurements described here, the bias is dropped across the two contacts on either side of the detector section under test, and the sign convention used is that of the potential of the contact closer to the surface of the pixel relative to the contact closer to the substrate. Thus, for example, for the MWIR section, the bias was applied to the top contact (see fig. 3) with the intermediate contact held at ground. Note that the coupled-well spectrum is substantially broader than that of the single-well sample. This is typical of a coupled-well system in which the ground and excited states are split into pairs of states, resulting in two dominant transitions that are convolved (but not resolved here).

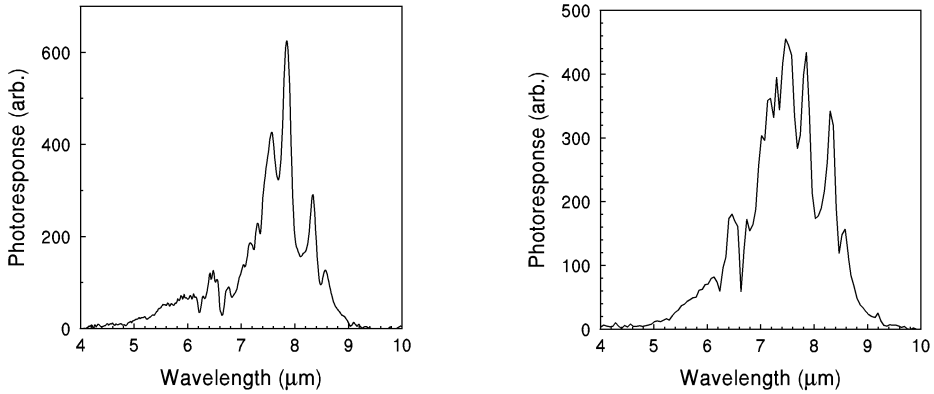

Figure 6. Relative response for the LWIR sections of the single-well (a) and the coupled-well (b) samples.

Figure 7 shows the relative photocurrent response versus wavelength for the MWIR sections of the single-well (a) and the coupled-well (b) samples at a bias of –1 V. Note that the coupled-well spectrum is not substantially different from the single-well spectrum. This indicates that the coupling between the wells in the coupled-well sample is relatively weak, and, at least optically, the pair of wells act as two independent absorbing wells.

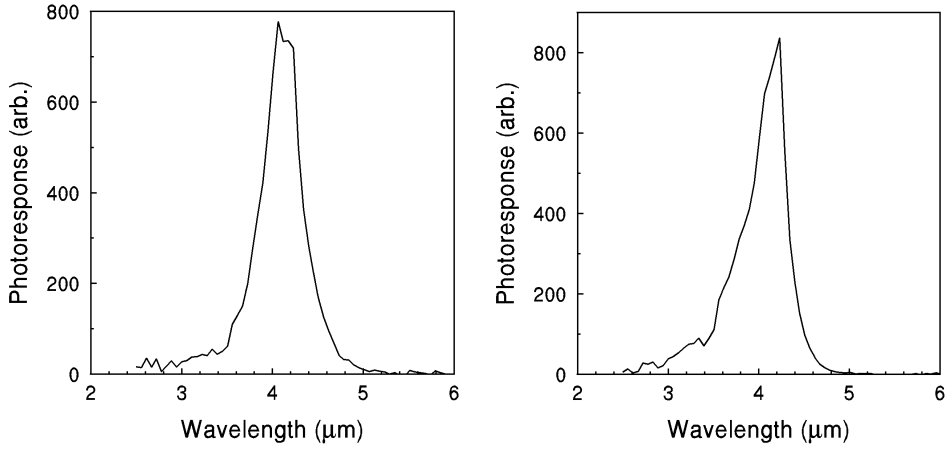

Figure 7. Relative response of the MWIR sections of the single-well (a) and the coupled-well (b) samples.

Figure 8 shows the spectral characteristics of the coupled-well sample operated as an independently addressable two-color detector. Note that there is no discernable cross-talk between the two bands indicating that this QWIP design would be very well suited for application in an LWIR/MWIR two-color imaging system.

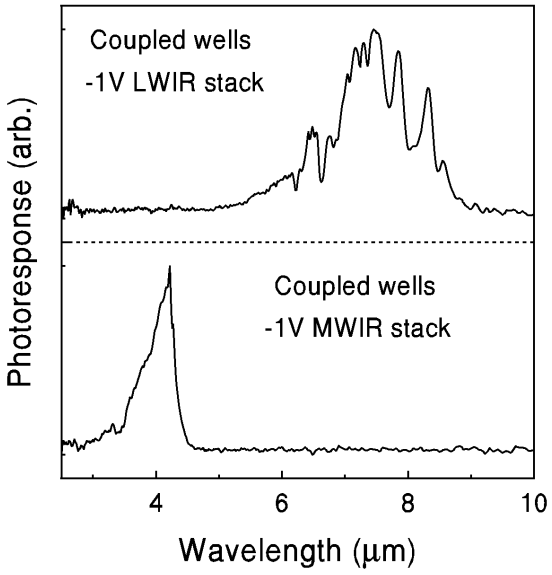

Figure 8. Relative response of the two stacks biased independently.

5.0 DARK CURRENT

The dewar used here has a cold shield surrounding the sample with an open aperture, which results in room temperature (300 K) illumination of the detector with an equivalent *f*-number of 2.5. The aperture can be blocked by a cold (78 K) shutter, which results in a 180° field of view of 78 K background radiation (i.e., the sample is essentially in the dark). Figure 9(a) and 9(b) show the absolute value of the current density vs. bias for typical LWIR and the MWIR sections, respectively, of the coupled well sample with and without the aperture blocked.

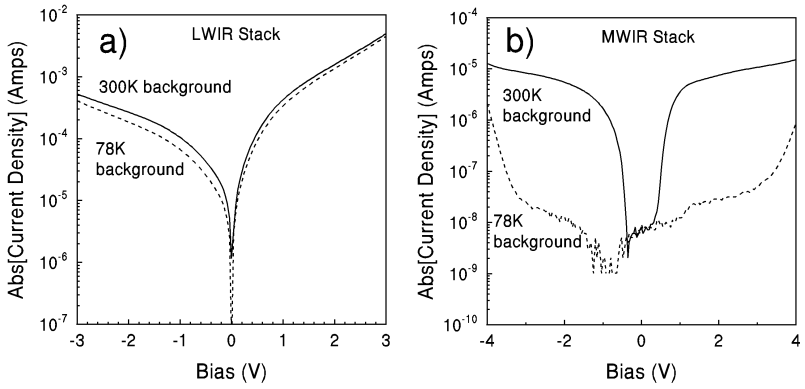

Figure 9. Absolute value of the current density for typical LWIR (a) and MWIR (b) sections in the dark and under 300 K illumination (*f*/2.5).

The slight increase in current density with 300 K illumination compared with 78 K in figure 9(a) indicates that the LWIR portion of the detector is partially background-limited at 78 K under *f*/2.5, 300 K background illumination. Figure 9(b) shows that the MWIR portion of the detector is essentially background-limited at 78 K, since the photocurrent density generated by 300 K illumination is more than 2 orders of magnitude greater than the dark current density. For the MWIR section, the absolute value of the current density reaches the system limit of around 2×10^{-9} A/cm^2 (indicating that the actual current changed sign) at a bias of about –1 V. This bias was different from pixel to pixel but was always a negative value. This could be an indication of a variation in a built-in field within the MWIR section, but it could also be explained by a slight positive offset current induced in the measurement system (e.g., by thermocouple currents in the dewar connections. Because the dynamic resistance is so high around zero bias (and thus the current versus bias curve is nearly flat), slight variations in the offset current would result in large variations in the bias at which the current changed sign.

If we compare the 78 K background curve shown in fig. 9(b) (i.e., the dark current density of the MWIR section at a sample temperature of 78 K) with the 78 K curves shown in fig.1 (which, when converted to current density for 100 x 100-μm^2 pixels, shows a range of 2×10^{-4} to 3×10^{-5} A/cm^2 at –1-V bias), we see that the dark current density for our sample is about 4 orders of magnitude lower than that for the MWIR sample described by fig. 1. This very low dark current is what would be expected for thermionic emission from the relatively deep well of an MWIR QWIP. Except for the variation in the zero crossing bias, all the pixels tested on our sample showed similar dark current curves.

Figure 10 shows the 300 K background current density versus bias that was measured in the MWIR sections of several pixels of the coupled-well sample. At an operating bias of, e.g., –2V, there is very little variation the background-limited dark current density, which is an important requirement for high performance in FPA applications.

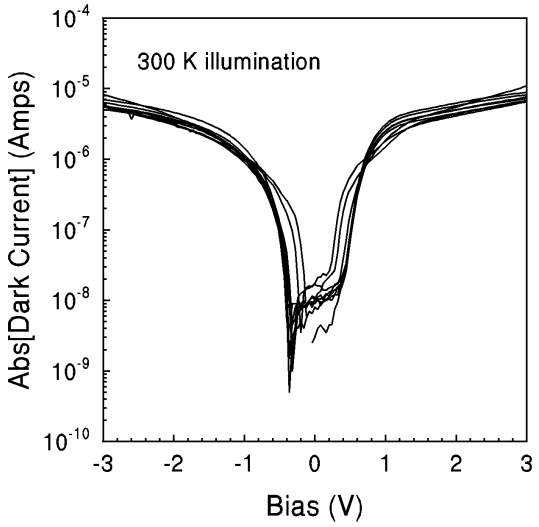

Figure 10. Current density for several coupled-well pixels under 300 K illumination.

6.0 RADIOMETRIC TEST RESULTS

6.1 RESPONSIVITY AND DETECTIVITY

The responsivity of a photodetector is a measure of the amount of photocurrent generated per unit optical power incident on the detector. We define the blackbody responsivity as

$$R_{bb} = \frac{R_p g(\lambda) P_{bb}(T,\lambda) d\lambda}{P_{bb}(T,\lambda) d\lambda} \quad (1)$$

where λ is the wavelength, R_p is the peak responsivity, $g(\lambda)$ is the normalized spectral response function, and $P_{bb}(T,\lambda)$ is the spectral power distribution function for a blackbody source at a temperature T. R_{bb} is the total photocurrent generated by a detector irradiated by a blackbody source at a temperature T, divided by the total power emitted by the blackbody source. For a given detector, the value of R_{bb} depends on the temperature of the blackbody source, whereas the peak responsivity does not. The blackbody detectivity is defined in terms of R_{bb} and the area A of the detector as

$$D^*_{bb} = \frac{R_{bb}(A\Delta f)^{1/2}}{i_n} \quad (2)$$

where i_n is the noise current measured over a frequency bandwidth of Δf. The peak detectivity, $D_p^*(\lambda_0)$ is given by equation 2 with R_{bb} replaced with R_p.

In general, the absorption in a QWIP is relatively weak and depends on the angle of incidence and polarization state of the light. The average intensity and the distribution of incidence angles and polarization states in a QWIP pixel depend critically on the geometry of the chip, the surrounding environment, and the nature of the light source and optical coupling structure. For example, the intensity of light that enters the chip at a well-defined angle (e.g., through a 45° polished facet) and strikes a pixel can be easily calculated. However, the relatively large fraction of the incident light that is not absorbed by the quantum wells on the first pass is typically confined inside the chip by total internal reflection at other surfaces. This excess light can eventually interact with the quantum wells again, increasing the average light intensity at the pixel by an amount that is not easily determined. Therefore, we must be very careful not to compare values of parameters such as responsivity, detectivity, and quantum efficiency that are determined under one set of experimental conditions with those that are obtained under a different set of conditions.

We have chosen a chip-mounting geometry (see fig. 4) that makes it convenient to independently obtain data from the two stacks of quantum wells under the same conditions of illumination. However, this is not a common geometry for general QWIP testing, and, therefore, the results presented here are most useful for comparing the performance of one color band to the other in the same pixel. Care must be taken that the conditions are reproduced as closely as possible if a comparison is made with data from another chip mounted and tested in the same way. These results cannot be directly compared with data from detectors that were tested under different circumstances.

The radiometric data were taken using a calibrated, chopped blackbody source with a 0.2-in. aperture positioned a fixed distance (about 35 cm) from the plane of the cold finger of the liquid nitrogen pour-fill dewar described above. For most of the tests reported here, the blackbody temperature was 800 K, the chopper frequency was 500 Hz, and the sample temperature was 78 K.

Figure 11 gives the blackbody responsivity (a) and blackbody detectivity (b) for both the LWIR and MWIR sections of a 70-µm square coupled-well detector pixel. To determine the detectivity shown in fig. 11(b), we needed to measure the noise current associated with the flow of current in the device (i.e., the shot noise). For the LWIR section, the measured noise was well above the noise floor of the measurement system, thus making the values fairly

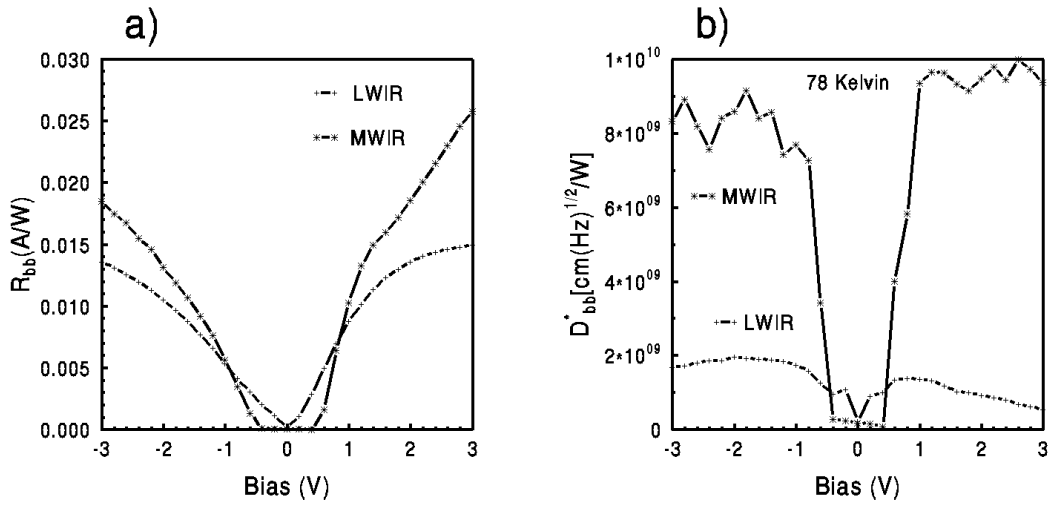

Figure 11. 800 K blackbody responsivity (a) and detectivity (b) for the coupled-well QWIP

reliable. However, the current flowing in the MWIR section (even under 300 K background illumination) is low enough that the maximum resulting noise was only about a factor of 2 above the noise floor. Therefore, the MWIR detectivity values and other parameters requiring noise measurements may not be as reliable.

Figure 12 gives the peak responsivity (a) and detectivity (b) for the two sections. These values are approximately a factor of 10 higher than the blackbody values, indicating that the overlap of both spectral bands with the 800 K blackbody power spectrum is about 0.1. The MWIR spectrum is close to the peak wavelength of the blackbody spectrum but it is relatively narrow. The LWIR spectrum is broader, but is more removed from the emission peak and contains the epoxy absorption spikes that remove integrated response. Even though the LWIR section contains twice as many quantum wells as the MWIR section, the peak responsivity of the MWIR section exceeds that of the LWIR section for absolute biases greater than about 1 V. As will be shown in the next section, this is due in large part to a much lower photoconductive gain in the LWIR stack than the MWIR stack.

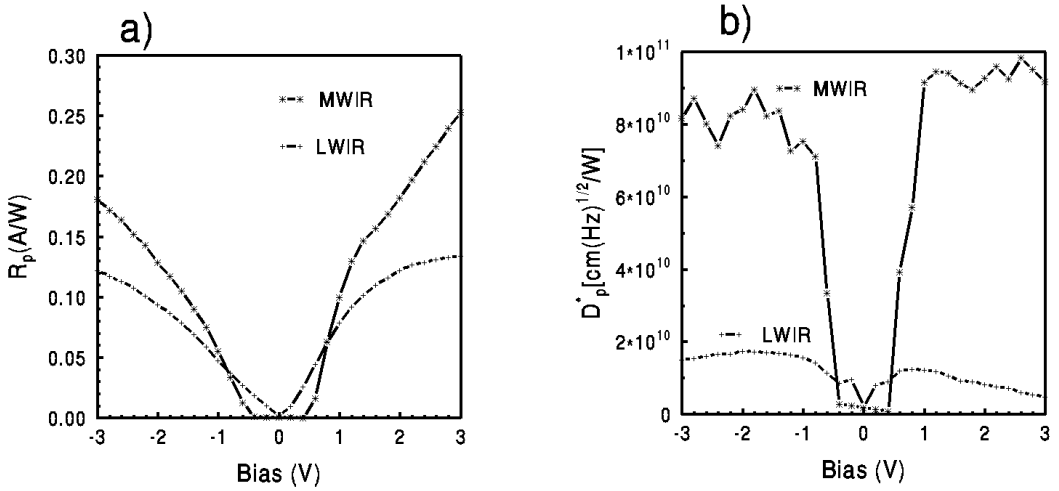

Figure 12. Peak responsivity (a) and detectivity (b) for the coupled-well QWIP

6.2 PHOTOCONDUCTIVE GAIN, CONVERSION EFFICIENCY, AND QUANTUM EFFICIENCY

The peak responsivity can be written as[13]

$$R_p = \frac{e\lambda_0}{hc}\eta g \tag{3}$$

where λ_0 is the peak response wavelength, e is the electronic charge, h is Plank's constant, c is the speed of light, η is the quantum efficiency, and g is the photoconductive gain. As defined here, the quantum efficiency is the probability that an incoming photon produces an electron in the conducting channel and, therefore, includes the probability that a photon is absorbed and the probability that a photoexcited electron is extracted from the quantum well (instead of decaying back to the ground state). The photoconductive gain is the ratio of the carrier transit time across one of the quantum wells to the characteristic time required for a carrier in the conducting channel to decay down to the ground state of a quantum well. This is equivalent to the number of quantum wells encountered by an electron in the conducting channel before it is trapped in a ground state divided by the total number of quantum wells in the sample. A gain less than unity means that more than one excitation event (e.g., absorbed photon or thermionic emission) must occur for an electron to travel the length of the sample, and a gain greater than unity means that each excited electron completes more than one complete circuit through the device.

Because the photoconductive gain affects the noise associated with current flow in the device, its value can be determined from the ratio of the measured noise power density to the full shot noise power density (as calculated from the measured current flowing in the device)[13]. Figure 13 shows the photoconductive gain determined for both sections of the two-color detector. Since inaccuracies increase as the noise level approaches the noise floor of the measurement system (as discussed above), the low-bias gain values for the LWIR section and all the values for the MWIR section show a substantial amount of scatter. However, the general features are that the gain for the LWIR

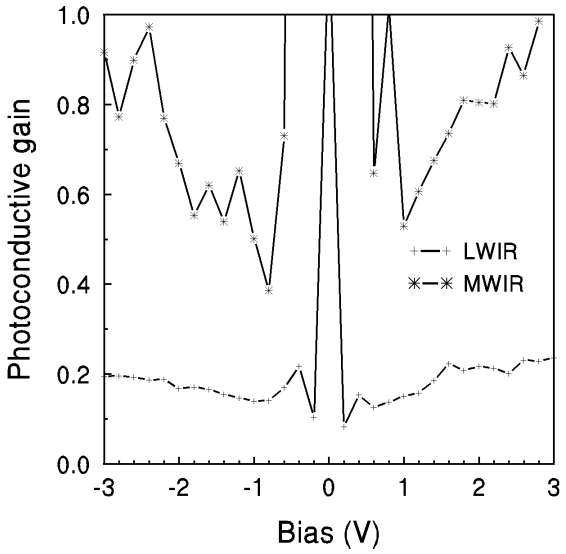

Figure 13. Photoconductive gain for the LWIR and MWIR sections of the coupled-well QWIP.

section is on the order of 0.2 with a weak bias dependence, and the gain for the MWIR section increases strongly with bias to a value approaching unity. The value of 0.2 for the LWIR section is very similar to that found for an

[13] K. K. Choi, "The Physics of Quantum Well Infrared Photodetectors, World Press, Singapore, 1997.

LWIR MBT detector with a total of 40 wells (the same total number as in this sample),[14] and the substantially higher gain for the BQB MWIR section of this sample is consistent with the values reported for an LWIR BQB (when scaled by the ratio of the number of quantum wells in the two samples).

The product of the quantum efficiency and the photoconductive gain is proportional to the amount of photocurrent generated by a single incoming photon and is referred to as the conversion efficiency (i.e., the photon is converted into photocurrent). The conversion efficiency can be determined from a measurement of the peak responsivity and the peak wavelength (see eq. (3)). The quantum efficiency can then be determined by dividing the conversion efficiency by the photoconductive gain. The conversion efficiencies and the quantum efficiencies for both sections are shown in figures 14(a) and 14(b), respectively. Note that the conversion efficiency of the MWIR section is about 5% and 7.5% at –3-V bias and +3-V bias, respectively, and is substantially higher than that of the LWIR section for nearly all biases. The quantum efficiency of the MWIR section is lower than that of the LWIR section. This is consistent with the factor of two fewer absorbing wells in the MWIR section than in the LWIR section. However, this quantum efficiency is not simply the absorption probability, but it includes the probability of extraction of the photocarriers from the well. We have not measured the extraction probability for these samples, but measurements on similar coupled-well samples[15] gave values that increased with increasing bias to a maximum value of about 0.8. It should also be reiterated that the LWIR response is lower than it should be due to absorption in the epoxy. Because of these conditions, it is difficult to interpret the data shown in fig. 14(b), except to say that the fundamental absorption efficiencies are at least as large as the quantum efficiencies given here.

7.0 TIME-DEPENDENT MWIR RESPONSE

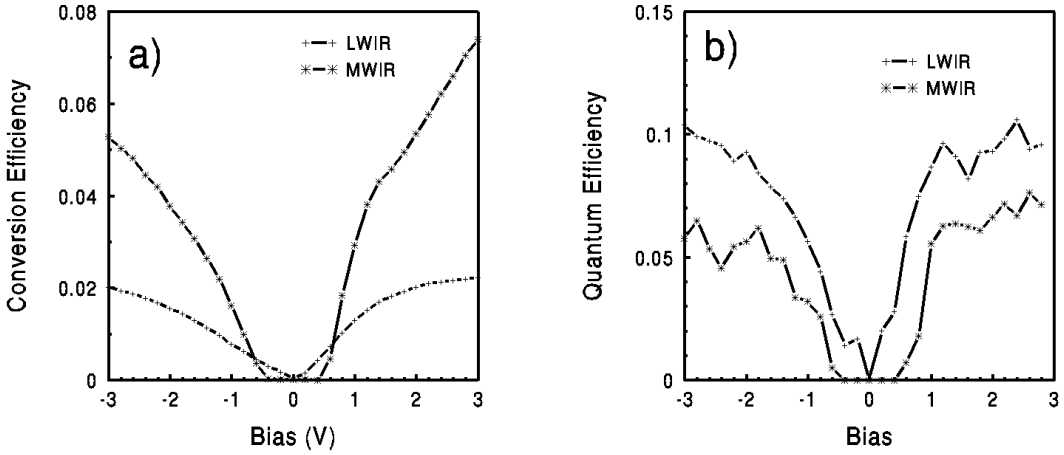

Figure 14. Conversion efficiency (a) and quantum efficiency (b) for the coupled-well QWIP. The quantum efficiency includes the probability of extracting the photocarrier from the well.

After the majority of the data presented above were taken using a chopper frequency of 500 Hz on the blackbody source, we noticed that the magnitude of the response of the MWIR section increased when the frequency of the chopper was decreased. This is indicative of a time-dependent response with a characteristic time constant

[14] S. W. Kennerly, J. W. Little, D. W. Beekman, R. P. Leavitt, and A. C. Goldberg, "Comparison of Bound to Quasibound and Miniband Transport Quantum Well Infrared Detector Structures," Proc. 1997 IRIS Specialty Group on Detectors, 1998.

[15] R. P. Leavitt, S. W. Kennerly, J. W. Little, D. W. Beekman, and A. C. Goldberg, "Determination of Optical Absorption Cross Sections and Photoelectron Escape Probabilities in Quantum Well Infrared Photodetectors," Proc. 21st Army Science Conference, 1998.

longer than the period of the chopped light. The LWIR section did not show this time dependence. An oscilloscope trace of the output of a current-sensitive preamp (connected in series with the detector) versus time showed that below about a 100-Hz chopper frequency, the waveform was trapezoidal in shape. This is indicative of a photocurrent output that followed the incident infrared intensity variation with time (i.e., of a finite source chopped with a sharp edge). However, above a 100-Hz chopper frequency, the waveform became more triangular (i.e., there was no region of constant photocurrent corresponding to the constant incident intensity), and the peak-to-peak magnitude decreased with increasing chopper frequency.

Figure 15(a) shows the –2-V MWIR photoresponse versus one-half of the chopper period (normalized to the magnitude of the response at 500 Hz, where all of the data presented above were taken). The horizontal axis represents the amount of time that the light is shining on the detector. The normalized response increases nearly linearly with time up to about 5 ms, where it begins to saturate at a value of about 1.8 (i.e., the response at the lower frequencies is about 1.8 times the response at 500 Hz). The saturation indicates that the photocurrent has reached a maximum. This implies that the detector has a response time to changes in the light intensity on the order of 5 ms.

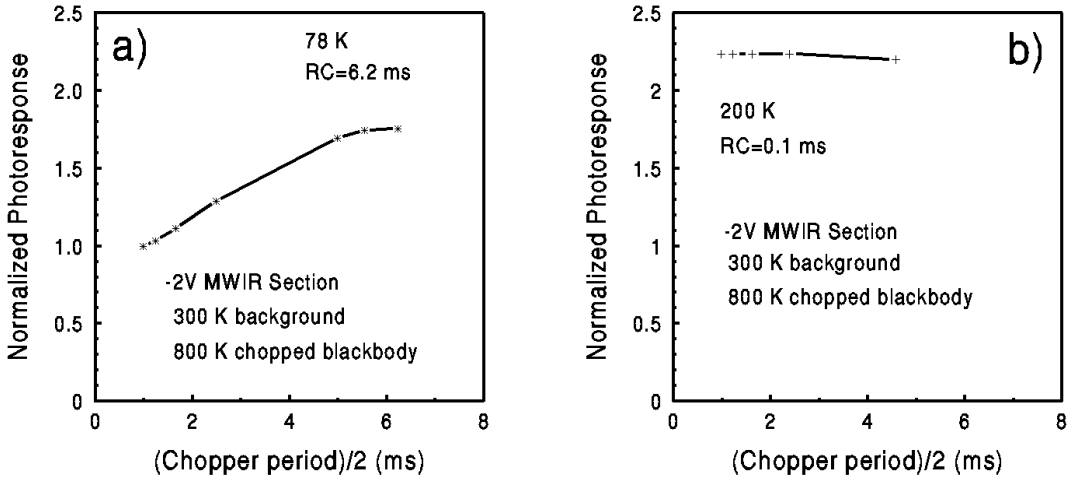

Figure 15. Normalized response of the MWIR section of the coupled-well QWIP as a function of the time the pixel was illuminated (one half of the chopper period) for a 78 K sample temperature (a) and a 200 K sample temperature (b).

Also shown in fig 15(a) is the calculated resistance-capacitance (RC) time constant for this device, where we have used the measured dynamic resistance of the device and the calculated capacitance[16] of a pair of heavily doped (essentially metallic) contacts separated by a material with a dielectric constant of 13.0[17] and a thickness equal to that of the MWIR stack. The rollover in the response corresponds quite well with the calculated RC time constant of the device.

The increase in response with decreasing frequency (below the 500 Hz used for data-taking) shown in fig. 15(a) implies that the intrinsic values of all of the parameters presented above that depend on the magnitude of the response (e.g., the responsivities, detectivities, conversion efficiencies, and quantum efficiencies) are larger by a factor of about 1.8 than those shown in the figures for the MWIR section.

[16] Franklin Miller, College Physics, Harcourt Brace Jovanovich, Inc., New York, 1977.
[17] Sadao Adachi, "GaAs, AlAs, and AlGaAs: Material parameters for Use in Research and Device Applications," J. Appl. Phys **58** (3), 1985.

Figure 15(b) shows the time-dependent response of the MWIR section (normalized to the 500-Hz, 78 K response) at a sample temperature of about 200 K. At this temperature, the dark current (and the dynamic resistance) is comparable to that of the LWIR section. The response is essentially independent of the chopper period, and the magnitude of the response is greater than the saturated response at 78 K. The RC time constant for the 200 K device is 0.1 ms and is much shorter than any of the illumination times used here. The constant response over the time periods examined would be expected from a sample with as short a time constant as the 200 K device. The increase in response at 200 K compared with the saturated 78 K response has been observes before,[18] and is attributed to enhanced carrier injection at the contacts for higher sample temperatures.

The elimination of the time-dependence of the response by the increase in the substrate temperature (and the corresponding reduction in the dynamic resistance and the RC time constant) suggests that a solution to the time constant problem is to decrease the device resistance. A reduction in the resistance of a factor of 10 would give a time constant of about 0.6 ms, which would be sufficient for most imaging applications. A simple increase in the doping density might be enough to accomplish the reduction in resistance (with an associated increase in responsivity), but there are practical limits to the doping density. We are studying other methods of tailoring the resistance of the device independent of the doping density (e.g., superlattice barriers with lower-lying minibands into which the deeply-bound ground state electrons can be thermally excited).

8.0 SUMMARY

We have designed, fabricated, and tested a new two-color LWIR/MWIR QWIP with features that address performance limitations in currently available designs. Uniform dark current was observed with no evidence of strain-related leakage currents. Radiometric tests showed good responsivities in both wavelength bands, with a substantial increase in the conversion efficiency of the MWIR section over that reported for current two-color QWIPs. A time dependence was observed in the high resistance MWIR response that was tentatively correlated with the RC time constant of the device. Further studies are underway to determine the source of the time dependence, and to find ways to eliminate it.

A wafer grown using essentially the same recipe described in this paper has been grown and is being transferred to ARL's industrial partners for fabrication of 256 x 256 two-color FPAs for comparison with existing arrays.

[18] A. C. Goldberg, J. W. Little, S. W. Kennerly, D. W. Beekman, and R. P. Leavitt, "Temperature Dependence of the Responsivity of QWIPs," Electrochemical Society Proc. 98-21.